Evaluation of ^{11}C-BU99008, a PET Ligand for the Imidazoline$_2$ Binding Site in Human Brain

Robin J. Tyacke[1], Jim F.M. Myers[1], Ashwin Venkataraman[1], Inge Mick[1], Samuel Turton[1], Jan Passchier[2], Stephen M. Husbands[3], Eugenii A. Rabiner[2], Roger N. Gunn[2,4], Philip S. Murphy[5], Christine A. Parker[1,5], and David J. Nutt[1]

[1]Neuropsychopharmacology Unit, Centre for Academic Psychiatry, Division of Brain Sciences, Imperial College London, London, United Kingdom; [2]Imanova Limited, Imperial College London, London, United Kingdom; [3]Department of Pharmacy and Pharmacology, University of Bath, Bath, United Kingdom; [4]Restorative Neurosciences, Imperial College London, London, United Kingdom; and [5]Experimental Medicine Imaging, GlaxoSmithKline Research and Development Limited, Stevenage, United Kingdom

The imidazoline$_2$ binding site (I_2BS) is thought to be expressed in glia and implicated in the regulation of glial fibrillary acidic protein. A PET ligand for this target would be important for the investigation of neurodegenerative and neuroinflammatory diseases. ^{11}C-BU99008 has previously been identified as a putative PET radioligand. Here, we present the first in vivo characterization of this PET radioligand in humans and assess its test–retest reproducibility. **Methods:** Fourteen healthy male volunteers underwent dynamic PET imaging with ^{11}C-BU99008 and arterial sampling. Six subjects were used in a test–retest assessment, and 8 were used in a pharmacologic evaluation, undergoing a second or third heterologous competition scan with the mixed I_2BS/α_2-adrenoceptor drug idazoxan (n = 8; 20, 40, 60, and 80 mg) and the mixed irreversible monoamine oxidase type A/B inhibitor isocarboxazid (n = 4; 50 mg). Regional time–activity data were generated from arterial plasma input functions corrected for metabolites using the most appropriate model to derive the outcome measure V_T (regional distribution volume). All image processing and kinetic analyses were performed in MIAKAT. **Results:** Brain uptake of ^{11}C-BU99008 was good, with reversible kinetics and a heterogeneous distribution consistent with known I_2BS expression. Model selection criteria indicated that the 2-tissue-compartment model was preferred. V_T estimates were high in the striatum (105 ± 21 mL·cm^{-3}), medium in the cingulate cortex (62 ± 10 mL·cm^{-3}), and low in the cerebellum (41 ± 7 mL·cm^{-3}). Test–retest reliability was reasonable. The uptake was dose-dependently reduced throughout the brain by pretreatment with idazoxan, with an average block across all regions of about 60% (V_T, ~30 mL·cm^{-3}) at the highest dose (80 mg). The median effective dose for idazoxan was 28 mg. Uptake was not blocked by pretreatment with the monoamine oxidase inhibitor isocarboxazid. **Conclusion:** ^{11}C-BU99008 in human PET studies demonstrates good brain delivery, reversible kinetics, heterogeneous distribution, specific binding signal consistent with I_2BS distribution, and good test–retest reliability.

Key Words: ^{11}C-BU99008; imidazoline$_2$ binding site; I_2BS, positron emission tomography; PET; BU99008

J Nucl Med 2018; 59:1597–1602
DOI: 10.2967/jnumed.118.208009

The ability of the α_2-adrenoceptor agonist clonidine and the antagonist idazoxan to label a subpopulation of binding sites that was not displaceable by the endogenous ligand noradrenaline led to the discovery of the imidazoline binding sites some 25 y ago (*1*). These binding sites have subsequently been divided into 3 groups: the imidazoline$_1$ binding site, which is preferentially labeled by ^{3}H-clonidine; the imidazoline$_2$ binding site (I_2BS), which is preferentially labeled by ^{3}H-idazoxan; and the imidazoline$_3$ binding site, which is an atypical imidazoline site found on pancreatic β-cells (*2*).

Changes in postmortem binding density of I_2BS have implicated it in a range of psychiatric conditions such as depression (*3,4*) and addiction (*5*), along with neurodegenerative disorders such as Alzheimer disease (*6*) and Huntington chorea (*7*). Functional interactions in preclinical models have also been demonstrated in relation to the opioid system, where I_2BS ligands have been shown to affect tolerance to morphine (*8,9*) and alleviate elements of the morphine withdrawal syndrome in rats (*10*). The location of I_2BS on glia and the possibility that it may in some way regulate glial fibrillary acidic protein (*11,12*) has led to increased interest in the role of I_2BS and I_2BS ligands in conditions characterized by marked gliosis. The density of I_2BS has been shown to increase in Alzheimer disease postmortem studies (*6*), and studies have also suggested that I_2BS may be a marker for human glioblastomas (*13*) and that in these tumors the increase seen in the maximum number of I_2BS binding sites may correlate with the severity and malignancy of the glioma (*14*). Subsequent work added weight to this argument, showing that the density of I_2BS increases in vivo with heat-induced gliosis (*15*).

PET is an in vivo imaging technique that uses radioligands as selective molecular probes to map the location and density of specific proteins. The development of a selective I_2BS PET radioligand would allow for the characterization of I_2BS in vivo and its regulation in disease states. Several ligands selective for I_2BS have been reported (*16*), but only 2 potential PET radioligands have

Received Jan. 10, 2018; revision accepted Feb. 21, 2018.
For correspondence or reprints contact: Robin J. Tyacke, Centre for Neuropsychopharmacology, Imperial College London, Burlington Danes Building, Hammersmith Hospital Campus, 160 Du Cane Rd., London W12 0NN, U.K.
E-mail: r.tyacke@imperial.ac.uk
Published online Mar. 9, 2018.

been reported to date: ^{11}C-benazoline has been synthesized (*17*) but not evaluated in vivo, and ^{11}C-FTIMD appears to have a low specific signal in rat and primate brain (*18,19*).

We have previously identified and evaluated ^{11}C-BU99008 as a putative I_2BS PET ligand in preclinical species (*20–22*). We have also shown that ^{11}C-BU99008 binds with a significantly lower affinity to monoamine oxidase (MAO) type B and thus is selective for I_2BS in these preclinical species. To meet the aims of this study and determine the regional density and distribution of I_2BS in healthy human brain, scans using ^{11}C-BU99008 were obtained in the presence and absence of 2 drugs, idazoxan and isocarboxazid.

Idazoxan is an α_2-adrenoceptor antagonist drug originally investigated in humans for its potential to treat psychiatric conditions (*23,24*). Defined as one of the archetypal I_2BS ligands, idazoxan has a high affinity for I_2BS, with an equilibrium dissociation constant of 20 and 13 nM in human cortical (*25*) and striatal (*26*) slices, respectively. Isocarboxazid is an irreversible, nonselective MAO inhibitor that has been in use for over 60 y and is well tolerated in humans (*27*). Although there is evidence that some I_2BS ligands also bind to MAO (*28*), ^{11}C-BU99008 shows very low affinity for MAO. Still, it is essential to know the contribution, if any, of a MAO-specific signal. Isocarboxazid was chosen because it will block both isoforms of MAO and has the lowest affinity for I_2BS of the available irreversible nonselective MAO inhibitors (*29*), thus minimizing any signal confounds.

We present the first, to our knowledge, in vivo evaluation and characterization of this ligand in healthy human volunteers using competition experiments to determine ^{11}C-BU99008 specificity and selectivity and assess its test–retest reproducibility.

MATERIALS AND METHODS

Radiochemistry

^{11}C-BU99008 was prepared by *N*-alkylation of the desmethyl precursor BU99007 using ^{11}C-CH_3I as previously described (*20,21*) (Supplemental Fig. 1; supplemental materials are available at http://jnm.snmjournals.org). The final formulation of the ^{11}C-BU99008 was in 20% EtOH/saline solution, affording a formulated intravenous preparation ready for dispensing and injection. Checks of chemical and radiochemical purity were performed, as well as analysis of the radiochemical yield and molar activity.

Blood and Metabolite Analysis

Analysis of ^{11}C-BU99008 metabolism in plasma was performed for each scan as follows: arterial blood samples were collected at 5, 10, 15, 20, 25, 30, 40, 50, 60, 70, 80, and 100 min after ^{11}C-BU99008 injection. Plasma samples were prepared, and the fraction of unchanged radioligand was determined using high-performance liquid chromatography by integration of the radioactivity peak corresponding to ^{11}C-BU99008 (retention time, ~6.5 min) and expressed as percentage of all radioactive peaks observed. The final plasma input function was calculated as the product of the total plasma curve and the parent fraction curve.

The free fraction of ^{11}C-BU99008 in plasma was measured through ultrafiltration (Amicon Ultra regenerated cellulose, molecular-weight cutoff of 30 kDa; Millex) in triplicate and compared with Tris buffer (0.1 M, pH 7.4) to enable correction for nonspecific filter binding.

Subjects

This PET study was performed at Imanova Centre for Imaging Sciences, London, U.K. The protocol for this study was approved by the national research ethics service (West London Research Ethics Committee; 14/LO/1741) and the national administration of radioactive substances advisory committee (630/3764/32214) and was conducted in accordance with good clinical practice guidelines, all applicable regulatory requirements, and the Code of Ethics of the World Medical

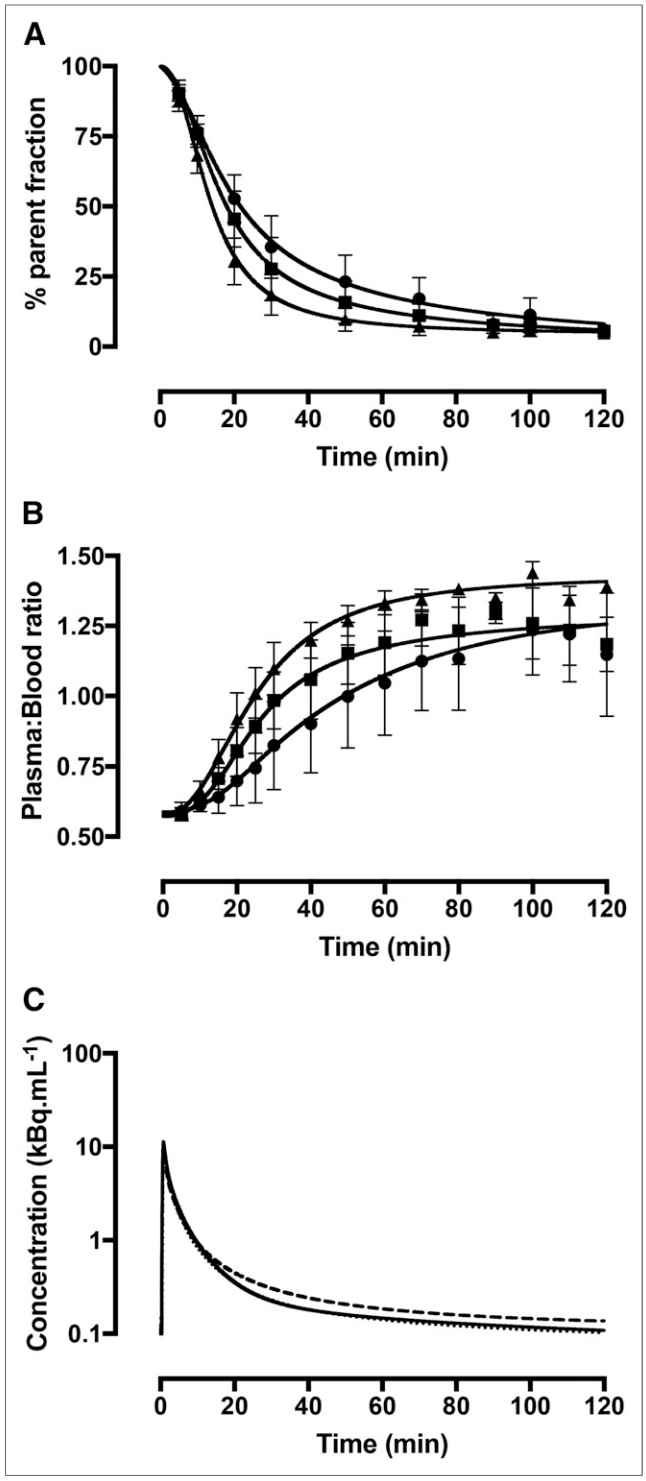

FIGURE 1. (A and B) Mean fits (sigmoid model) for parent fraction (A) and plasma-to-blood ratio (B) for unblocked scans (●), idazoxan-blocked scans (■), and isocarboxazid scans (▲). Vertical bars represent SD. (C) Calculated parent plasma input function (triexponential) for unblocked scans (solid line), idazoxan-blocked scans (dashed line), and isocarboxazid scans (dotted line).

Association (Declaration of Helsinki). All subjects provided written informed consent. The study, "Imidazoline2 Binding Site in Healthy Volunteers (I2PETHV)," was registered on the clinical trials database, identifier NCT02323217.

Heterologous Competition

Eight healthy male volunteers (aged 52 ± 8 y) underwent either 2 or 3 PET/CT scans with ^{11}C-BU99008 (120 min; specific activity, 50.6 ± 20.1 GBq·μmol^{-1}; injected dose, 308 ± 14 MBq; mass, 1.7 ± 1.7 μg) in a fixed-order open-label design. The first was a baseline scan with ^{11}C-BU99008 (n = 8). Later that day, the volunteers underwent a second PET/CT scan with ^{11}C-BU99008 120 min after an oral dose of the mixed I_2BS/α_2-adrenoceptor drug idazoxan (20, 40, 60, and 80 mg; n = 2 for each dose). At least 1 wk later, 4 of the 8 volunteers underwent a third PET/CT scan with ^{11}C-BU99008 (n = 4) 240 min after an oral dose of the mixed irreversible MAO type A/B inhibitor isocarboxazid (50 mg). Idazoxan was synthesized by Onyx Pharmaceuticals Inc., and isocarboxazid was purchased from a pharmaceutical supplier (Supplemental Table 1).

Test–Retest Reproducibility

Six further healthy male volunteers (aged 56 ± 6 y) underwent 2 PET/CT scans with ^{11}C-BU99008 (120 min; specific activity, 35.3 ± 17.5 GBq·μmol^{-1}; injected dose, 313.9 ± 11 MBq; mass, 2.9 ± 2.5 μg) at least 1 wk apart to determine the test–retest reproducibility of the radioligand quantification.

In both the specificity and the selectivity, and the test–retest experiments, the healthy volunteers' heart rate and blood pressure were monitored before, during, and after each PET/CT scan (Supplemental Table 1).

MRI

To enable accurate anatomic parcellation of the PET data, each volunteer also underwent T1-weighted structural MRI (3-T Magnetom Trio, syngo MR B13; Siemens Medical Solutions) for atlas-based region-of-interest (ROI) delineation.

PET Imaging

PET scans were acquired for 120 min on a HiRez Biograph 6 PET/CT scanner (Siemens Healthcare) and reconstructed into 29 frames (8 × 15, 3 × 60, 5 × 120, 5 × 300, 8 × 600 s) using filtered backprojection. Dynamic images were corrected for motion using a mutual information coregistration algorithm with frame 16 as the reference. Immediately before use, ^{11}C-BU99008 was manufactured at Imanova Centre for Imaging Sciences according to local standard operating procedures for good-manufacturing-practice production. ^{11}C-BU99008 was then injected as an intravenous bolus over approximately 20 s, and the PET emission data were collected. An arterial line was placed in all subjects, and blood was sampled continuously for 15 min. In addition, discrete blood samples were manually withdrawn at 5, 10, 15, 20, 25, 30, 40, 50, 60, 70, 80, 90, 100, 110, and 120 min after ^{11}C-BU99008 injection. Arterial blood radioactivity could then be converted to a total plasma concentration and corrected by the parent fraction to determine a parent plasma input function. CT data were also collected for attenuation-correction purposes.

Regional Time–Activity Curve Sampling and Modeling

All image processing and kinetic analyses were performed using MIAKAT (www.miakat.org). MRI structural data and PET data were coregistered into a mutual space, and the nonlinear registration of a standard Montreal Neurological Institute template to the structural image provided the parameters to warp the CIC atlas (*30*). This step permitted regional sampling of the PET data and generation of motion-corrected time–activity data for selected ROIs.

Parent plasma input functions were derived from the arterial blood measurements. The whole-blood data were corrected for plasma and metabolite fractions using sigmoid models and were interpolated with a triexponential function. These were used as input functions to a 1-tissue-compartment model, a 2-tissue-compartment model (with both fixed and fitted blood volume), and a multilinear analysis model (*31*). The most appropriate model was selected using the Akaike Information Criterion and percentage reliability (test–retest variability, calculated using

TABLE 1
Outcome Measures for Selected ROIs Using the 3 Models

	V_T ± SD* (mL·cm^{-3})			AIC*		Test–retest variability†		
ROI	1TCM	2TCM	MA	1TCM	2TCM	1TCM	2TCM	MA
Whole brain	44.5 ± 6.1	48.8 ± 7.9	44.8 ± 6.1	−237	−328	12.9	6.4	13.4
Cerebellum	39.3 ± 6.2	41.9 ± 6.9	39.6 ± 6.2	−237	−310	14.6	10.8	14.9
Brain stem	62.7 ± 9.1	66.4 ± 10.1	63.2 ± 9.2	−252	−276	13.7	11.7	14.6
Occipital lobe	38.6 ± 6.5	42.7 ± 8.6	38.8 ± 6.5	−234	−323	12.8	8.1	13.3
Insula	63.3 ± 9.0	67.7 ± 11.8	63.9 ± 9.1	−224	−267	14.6	11.0	14.8
Frontal lobe	41.6 ± 5.9	45.7 ± 7.9	42.0 ± 5.9	−225	−316	12.6	4.7	13.1
Cingulate	58.3 ± 8.6	62.2 ± 9.7	58.8 ± 8.6	−222	−293	14.6	10.2	15.1
Parietal lobe	39.2 ± 5.8	43.6 ± 8.7	39.5 ± 5.9	−233	−318	12.4	5.6	12.8
Amygdala	89.8 ± 15.2	94.6 ± 20.3	91.1 ± 15.1	−233	−242	23.2	24.7	23.3
Hippocampus	68.4 ± 11.4	77.7 ± 24.2	69.1 ± 11.5	−225	−264	16.1	15.9	16.4
Striatum	102.7 ± 17.8	105.7 ± 21.0	104.2 ± 17.6	−246	−259	16.9	16.7	17.4
Thalamus	75.3 ± 11.0	80.0 ± 14.1	76.0 ± 11.1	−228	−264	14.6	9.5	15.2

*n = 14.
†n = 5.
AIC = Akaike Information Criterion; 1TCM = 1-tissue-compartment model; 2TCM = 2-tissue-compartment model; MA = multilinear analysis model.

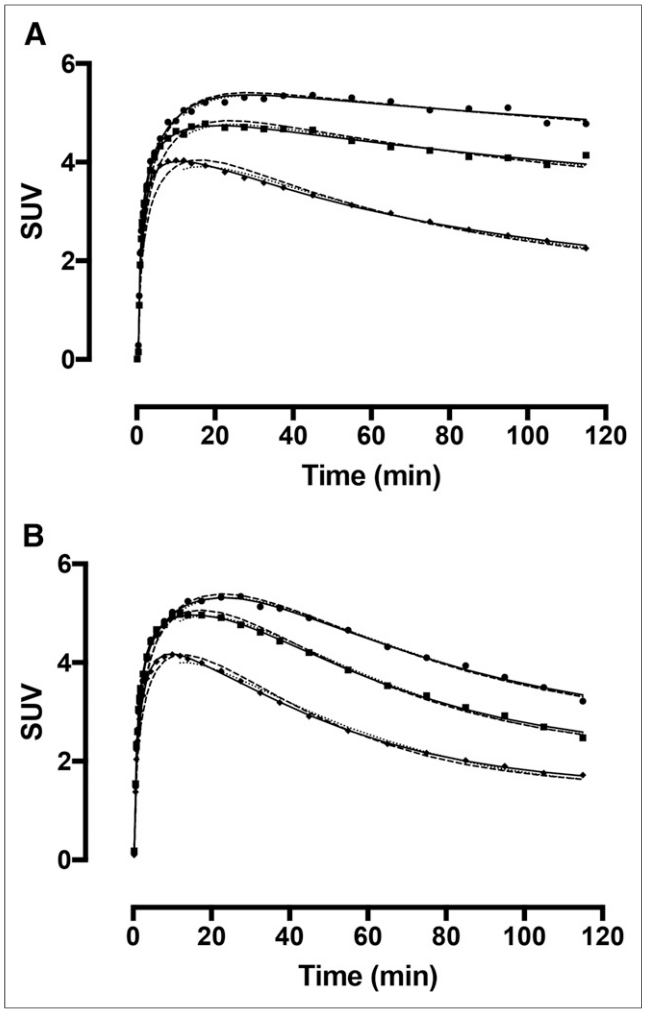

FIGURE 2. Representative time–activity curves for ^{11}C-BU99008 uptake into human brain at baseline (A) and after partial blockade by treatment with 80 mg of idazoxan (B) in striatum (•), thalamus (▪), and cerebellum (♦). Dashed line = 1-tissue-compartment model; solid line = 2-tissue-compartment model; dotted line = multilinear analysis model.

Eq. 1). It was found that there was no suitable reference tissue; the nondisplaceable volume of distribution and receptor occupancy were calculated using the occupancy plot (*32*).

$$\text{Variability} = \frac{100}{N}\sum_{i=1}^{N}\frac{|\text{test}_i - \text{retest}_i|}{|\text{test}_i + \text{retest}_i|/2} \qquad \text{Eq. 1}$$

RESULTS

Radiochemistry

^{11}C-BU99008 was successfully synthesized, with a radiochemical purity of 100% at the end of synthesis. The specific activity was 44.8 ± 19 GBq·μmol^{-1}, and an average mass of 2.1 ± 2.1 μg and radioactive dose of 310 ± 13.3 MBq were injected for all the syntheses/administrations. The identity of the radiolabeled material was confirmed by coinjection with a sample of authentic BU99008, which, under the same elution conditions, showed an identical retention time. A complete description of the ^{11}C-BU99008 parameters is provided as Supplemental Table 1.

Regional Time–Activity Curve Computation and Modeling

Brain uptake of ^{11}C-BU99008 was rapid, with reversible kinetics and a heterogeneous distribution consistent with known I_2BS expression (*20,21*). The arterial blood samples were used to determine a plasma input function (Fig. 1) to enable modeling of the time–activity curves and estimation of the volume of distribution (V_T). ^{11}C-BU99008 was metabolized such that approximately 10% of the parent radioligand remained in plasma at 120 min for all scans regardless of intervention.

When the Akaike Information Criterion (Table 1) and the robustness of fits in a selection of ROIs were compared between the 1- and 2-tissue-compartment models, the 2-tissue-compartment model, with a fixed 5% blood volume, seemed the more appropriate. When test–retest variability (within-subject; Eq. 1) in these ROIs was compared among all 3 models, the 2-tissue-compartment model again showed the greatest reliability. As a result, this model was used to estimate the V_T. The robust nature of the multilinear analysis model suggests it remains an option for a voxelwise analytical approach with this tracer, and although modulation of t^* has little effect on the outcome measure with this model, a differing regional underestimation of V_T between this model and the 2-tissue-compartment model may be noted.

Distribution and Heterologous Competition

Peak radioactive concentrations were observed approximately 10–20 min after administration of ^{11}C-BU99008, followed by a slow washout from all regions (Fig. 2). The uptake was highest in the striatum (V_T, 105.7 ± 21.0 mL·cm^{-3}) and lowest in the cerebellum (V_T, 41.9 ± 6.9 mL·cm^{-3}) (Table 1). The regional uptake in humans correlated well with that seen preclinically in pigs (r = 0.71; $P < 0.05$) and nonhuman primates (r = 0.84; $P < 0.05$). ^{11}C-BU99008 V_T was dose-dependently reduced by pretreatment with an oral dose of the mixed I_2BS/α_2-adrenoceptor drug idazoxan, with an average block across all regions of approximately 60% at the highest dose (80 mg; Figs. 3 and 4). No regions were devoid of blockade, indicating that no suitable reference tissue exists for this ligand. Pretreatment with the mixed irreversible MAO type A/B inhibitor isocarboxazid caused no reduction in V_T (Supplemental Fig. 2).

The global occupancy for each competition scan was calculated using the occupancy plot (Fig. 5) (*32*), and the resultant occupancy values were used to calculate the in vivo median effective dose of idazoxan (Fig. 5, inset). Occupancy varied greatly, ranging from approximately 20% at 20 mg to 80% at 80 mg, although for 2

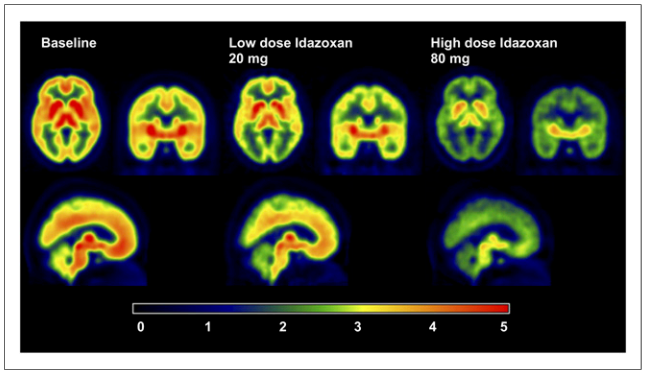

FIGURE 3. SUV images demonstrating heterogeneous brain uptake in all regions and dose-dependent blockade by idazoxan.

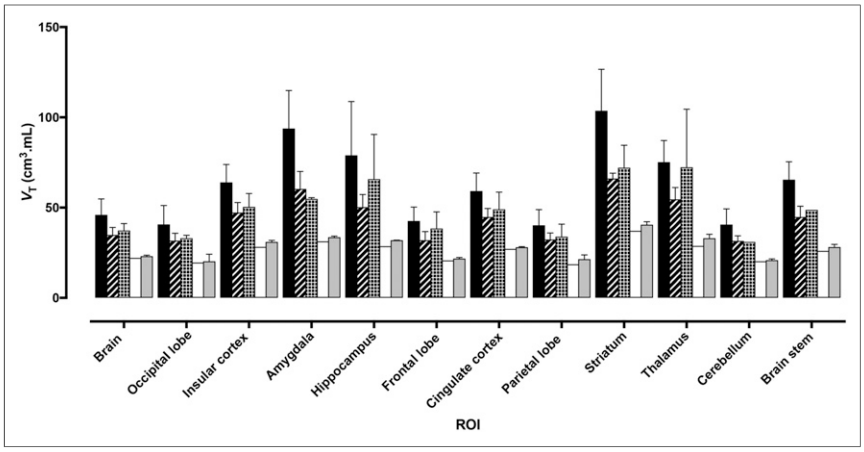

FIGURE 4. Bar chart showing V_T of ^{11}C-BU99008 and effect of increasing doses of the mixed I_2BS/α_2-adrenoceptor ligand idazoxan. From left to right, each set of bars is mean ± SD for baseline, for 20-mg dose, for 40-mg dose, for 60-mg dose, and for 80-mg dose. Bars represent mean ± SD. Data are from a selection of representative brain regions.

individuals the occupancy was apparently negligible. The median effective dose of idazoxan was 0.27 mg·kg^{-1}, and the estimated nondisplaceable distribution volume was 19.2 mL·cm^{-3} (Fig. 5).

Test–Retest Variability

Because of a technical failure of the well counter, blood data were not fully collected for 1 retest scan; thus, test–retest data were available from only 5 subjects. Test–retest variability was reasonable, though quite high in several regions (above 10% in most subcortical and limbic regions). The ligand performed better throughout the cortex (Table 1; Supplemental Fig. 3).

DISCUSSION

We present the characterization of the novel I_2BS PET radioligand ^{11}C-BU99008 in vivo in humans. In this study, ^{11}C-BU99008 demonstrated a high specific signal in the brain, defined by blockade of I_2BS by idazoxan, along with reliable compartmental modeling and good selectivity.

The competition study had some limitations, including the relatively few subjects, the restricted dose range due to the limited tolerability of idazoxan (maximum dose, 80 mg), and, consequently, the restricted level to which the PET radioligand might be blocked. The restricted dose range makes in vivo estimation of the median effective dose quite difficult, though we were encouraged to see such a clear dose response over the range that we provided. The stability of occupancy measures at these doses is hard to estimate, but one should note that idazoxan had little effect in 2 subjects, perhaps because of differing metabolism of the drug. This possibility could have been clarified by taking plasma concentration measurements, but we did not have this option during the study. In addition, these limitations make the nature of the idazoxan blockade difficult to determine. The reduction in V_T by the various doses of idazoxan in Figure 4 is not as obvious as might have been hoped. Some higher doses appear not to block as much of the ^{11}C-BU99008 binding as lower doses. One possible reason is a biphasic blockade by idazoxan. Unfortunately, the small numbers in this experiment do not allow this possibility to be fully explored. Considering these data in combination with the global occupancy and the generated dose–response curve (Fig. 5), the simpler, more conservative monophasic model of blockade is more appropriate.

There was some degree of test–retest variability, between 15% and 25%, in the outcome measure in subcortical regions, particularly the amygdala, striatum, and other relatively high-binding structures. A possible explanation is the slow kinetics of the ligand, consistent with a high V_T. As we scanned for 2 h, beyond which an ^{11}C signal is no longer robust, the kinetics will make it difficult to demonstrate group differences in subcortical ROIs unless the effect is large or the groups are large. The kinetics are not, however, prohibitive, and the strong and robust cortical signal is encouraging.

The lack of any reduction in signal after mixed MAO type A/B inhibition with isocarboxazid suggests that ^{11}C-BU99008 has no significant off-target binding to MAO in humans. The idazoxan competition study gave a consistent nondisplaceable distribution volume of 19.2 mL·cm^{-3}, which represents about half the total distribution volume in the lowest-binding region (cerebellum) and less than 20% of the signal in the regions with the highest binding. Thus, the specific signal is generally high throughout the brain, with nondisplaceable binding potentials (estimated from the 2-tissue-compartment model as k_3/k_4) ranging from 1 to 4.

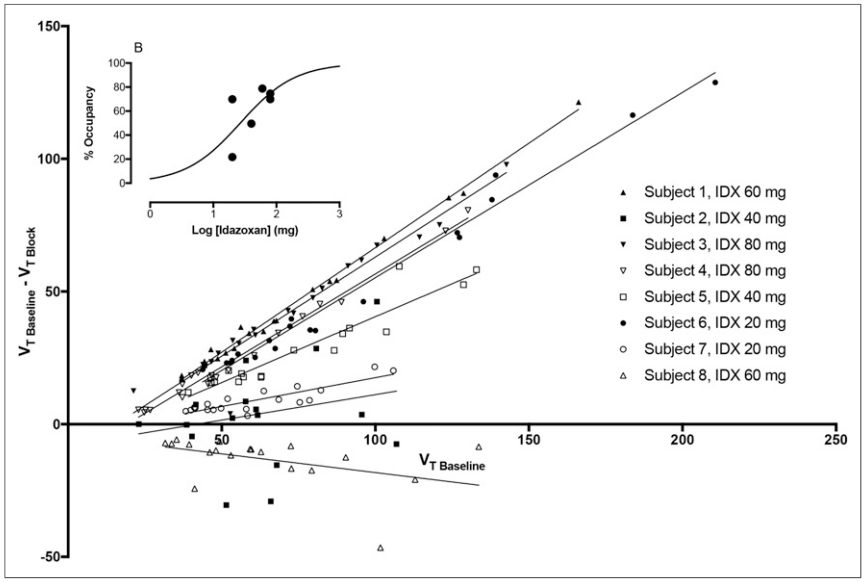

FIGURE 5. Occupancy plots for subjects in heterologous block study, along with dose–response curve for individuals in whom occupancy was observed (inset). Median effective dose was 27.7 mg or 0.27 mg·kg^{-1}, and estimated nondisplaceable distribution volume was 19.2 mL·cm^{-3}.

CONCLUSION

^{11}C-BU99008 PET can image I_2BS with high specificity and selectivity, enabling investigation of the function of I_2BS in the living human brain and in disease states with which I_2BS is known to be associated. This new clinical imaging tool has paved the way for more in-depth clinical investigations into the role of I_2BS in disease states and in the development of potential therapies.

DISCLOSURE

This study was funded jointly by GSK and the MRC (MR/L01307X/1). We present independent research supported by the NIHR CRF at Imperial College Healthcare NHS Trust. The views expressed are those of the authors and not necessarily those of the MRC, the NHS, the NIHR, or the Department of Health. No other potential conflict of interest relevant to this article was reported.

ACKNOWLEDGMENTS

We thank the Imanova Centre for Imaging Sciences for performing all PET syntheses and scans and providing logistical, technical, and analytical support.

REFERENCES

1. Regunathan S, Feinstein DL, Reis DJ. Expression of non-adrenergic imidazoline sites in rat cerebral cortical astrocytes. *J Neurosci Res.* 1993;34:681–688.
2. Morgan NG, Chan SL, Brown CA, Tsoli E. Characterization of the imidazoline binding site involved in regulation of insulin secretion. *Ann N Y Acad Sci.* 1995; 763:361–373.
3. Finn DP, Marti O, Harbuz MS, et al. Behavioral, neuroendocrine and neurochemical effects of the imidazoline I_2 receptor selective ligand BU224 in naive rats and rats exposed to the stress of the forced swim test. *Psychopharmacology (Berl).* 2003;167:195–202.
4. García-Sevilla JA, Escriba PV, Sastre M, et al. Immunodetection and quantitation of imidazoline receptor proteins in platelets of patients with major depression and in brains of suicide victims. *Arch Gen Psychiatry.* 1996;53:803–810.
5. Sastre M, Ventayol P, Garcia-Sevilla JA. Decreased density of I2-imidazoline receptors in the postmortem brain of heroin addicts. *Neuroreport.* 1996;7:509–512.
6. García-Sevilla JA, Escriba PV, Walzer C, Bouras C, Guimon J. Imidazoline receptor proteins in brains of patients with Alzheimer's disease. *Neurosci Lett.* 1998;247:95–98.
7. Reynolds GP, Boulton RM, Pearson SJ, Hudson AL, Nutt DJ. Imidazoline binding sites in Huntington's and Parkinson's disease putamen. *Eur J Pharmacol.* 1996; 301:R19–R21.
8. Ruiz-Durántez E, Torrecilla M, Pineda J, Ugedo L. Attenuation of acute and chronic effects of morphine by the imidazoline receptor ligand 2-(2-benzofuranyl)-2-imidazoline in rat locus coeruleus neurons. *Br J Pharmacol.* 2003;138:494–500.
9. Boronat MA, Olmos G, Garcia-Sevilla JA. Attenuation of tolerance to opioid-induced antinociception and protection against morphine-induced decrease of neurofilament proteins by idazoxan and other I_2-imidazoline ligands. *Br J Pharmacol.* 1998;125:175–185.
10. Hudson AL, Gough R, Tyacke R, et al. Novel selective compounds for the investigation of imidazoline receptors. *Ann N Y Acad Sci.* 1999;881:81–91.
11. Casanovas A, Olmos G, Ribera J, Boronat MA, Esquerda JE, Garcia-Sevilla JA. Induction of reactive astrocytosis and prevention of motoneuron cell death by the I_2-imidazoline receptor ligand LSL 60101. *Br J Pharmacol.* 2000;130:1767–1776.
12. Olmos G, Alemany R, Escriba PV, Garcia-Sevilla JA. The effects of chronic imidazoline drug treatment on glial fibrillary acidic protein concentrations in rat brain. *Br J Pharmacol.* 1994;111:997–1002.
13. Martín-Gómez JI, Ruiz J, Callado LF, et al. Increased density of I2-imidazoline receptors in human glioblastomas. *Neuroreport.* 1996;7:1393–1396.
14. Callado LF, Martin-Gomez JI, Ruiz J, Garibi JM, Meana JJ. Imidazoline I_2 receptor density increases with the malignancy of human gliomas. *J Neurol Neurosurg Psychiatry.* 2004;75:785–787.
15. Martín-Gómez JI, Ruiz J, Barrondo S, Callado LF, Meana JJ. Opposite changes in imidazoline I_2 receptors and α_2-adrenoceptors density in rat frontal cortex after induced gliosis. *Life Sci.* 2005;78:205–209.
16. Dardonville C, Rozas I. Imidazoline binding sites and their ligands: an overview of the different chemical structures. *Med Res Rev.* 2004;24:639–661.
17. Roeda D, Hinnen F, Dolle F. Radiosynthesis of a 2-substituted 4,5-dihydro-^{1}H-[2-^{11}C] imidazole: the I_2 imidazoline receptor ligand [^{11}C] benazoline. *J Labelled Comp Radiopharm.* 2003;46:1141–1149.
18. Kawamura K, Kimura Y, Yui J, et al. PET study using [^{11}C]FTIMD with ultra-high specific activity to evaluate I_2-imidazoline receptors binding in rat brains. *Nucl Med Biol.* 2012;39:199–206.
19. Kawamura K, Naganawa M, Konno F, et al. Imaging of I_2-imidazoline receptors by small-animal PET using 2-(3-fluoro-[4-^{11}C]tolyl)-4,5-dihydro-^{1}H-imidazole ([^{11}C]FTIMD). *Nucl Med Biol.* 2010;37:625–635.
20. Kealey S, Turner EM, Husbands SM, et al. Imaging imidazoline-I_2 binding sites in porcine brain using ^{11}C-BU99008. *J Nucl Med.* 2013;54:139–144.
21. Parker CA, Nabulsi N, Holden D, et al. Evaluation of ^{11}C-BU99008, a PET ligand for the imidazoline$_2$ binding sites in rhesus brain. *J Nucl Med.* 2014;55:838–844.
22. Tyacke RJ, Fisher A, Robinson ES, et al. Evaluation and initial in vitro and ex vivo characterization of the potential positron emission tomography ligand, BU99008 (2-(4,5-dihydro-^{1}H-imidazol-2-yl)-1-methyl-^{1}H-indole), for the imidazoline$_2$ binding site. *Synapse.* 2012;66:542–551.
23. Litman RE, Su TP, Potter WZ, Hong WW, Pickar D. Idazoxan and response to typical neuroleptics in treatment-resistant schizophrenia: comparison with the atypical neuroleptic, clozapine. *Br J Psychiatry.* 1996;168:571–579.
24. Osman OT, Rudorfer MV, Potter WZ. Idazoxan: a selective α2-antagonist and effective sustained antidepressant in two bipolar depressed patients. *Arch Gen Psychiatry.* 1989;46:958–959.
25. De Vos H, Convents A, De Keyser J, et al. Autoradiographic distribution of α_2 adrenoceptors, NAIBS, and 5-HT_{1A} receptors in human brain using [^{3}H]idazoxan and [^{3}H]rauwolscine. *Brain Res.* 1991;566:13–20.
26. De Vos H, Bricca G, De Keyser J, De Backer JP, Bousquet P, Vauquelin G. Imidazoline receptors, non-adrenergic idazoxan binding sites and α_2-adrenoceptors in the human central nervous system. *Neuroscience.* 1994;59:589–598.
27. Davidson J, Turnbull C. Isocarboxazid. Efficacy and tolerance. *J Affect Disord.* 1983;5:183–189.
28. Eglen RM, Hudson AL, Kendall DA, et al. 'Seeing through a glass darkly': casting light on imidazoline 'I' sites. *Trends Pharmacol Sci.* 1998;19:381–390.
29. Alemany R, Olmos G, Garcia-Sevilla JA. The effects of phenelzine and other monoamine oxidase inhibitor antidepressants on brain and liver I_2 imidazoline-preferring receptors. *Br J Pharmacol.* 1995;114:837–845.
30. Tziortzi AC, Searle GE, Tzimopoulou S, et al. Imaging dopamine receptors in humans with [^{11}C]-(+)-PHNO: dissection of D3 signal and anatomy. *Neuroimage.* 2011;54:264–277.
31. Ichise M, Toyama H, Innis RB, Carson RE. Strategies to improve neuroreceptor parameter estimation by linear regression analysis. *J Cereb Blood Flow Metab.* 2002;22:1271–1281.
32. Cunningham VJ, Rabiner EA, Slifstein M, Laruelle M, Gunn RN. Measuring drug occupancy in the absence of a reference region: the Lassen plot re-visited. *J Cereb Blood Flow Metab.* 2010;30:46–50.